Smart aggregates: multi-functional sensors for concrete structures—a tutorial and a review

TOPICAL REVIEW

Smart aggregates: multi-functional sensors for concrete structures—a tutorial and a review

Gangbing Song[1,3], Haichang Gu[1] and Yi-Lung Mo[2]

[1] Department of Mechanical Engineering, University of Houston, Houston, TX 77204, USA
[2] Department of Civil and Environmental Engineering, University of Houston, Houston, TX 77204, USA

E-mail: gsong@uh.edu

Abstract

This paper summarizes the authors' recent pioneering research work in piezoceramic-based smart aggregates and their innovative applications in concrete civil structures. The basic operating principle of smart aggregates is first introduced. The proposed smart aggregate is formed by embedding a waterproof piezoelectric patch with lead wires into a small concrete block. The proposed smart aggregates are multi-functional and can perform three major tasks: early-age concrete strength monitoring, impact detection and structural health monitoring. The proposed smart aggregates are embedded into the desired location before the casting of the concrete structure. The concrete strength development is monitored by observing the high frequency harmonic wave response of the smart aggregate. Impact on the concrete structure is detected by observing the open-circuit voltage of the piezoceramic patch in the smart aggregate. For structural health monitoring purposes, a smart aggregate-based active sensing system is designed for the concrete structure. Wavelet packet analysis is used as a signal-processing tool to analyze the sensor signal. A damage index based on the wavelet packet analysis is used to determine the structural health status. To better describe the time-history and location information of damage, two types of damage index matrices are proposed: a sensor-history damage index matrix and an actuator–sensor damage index matrix. To demonstrate the multi-functionality of the proposed smart aggregates, different types of concrete structures have been used as test objects, including concrete bridge bent-caps, concrete cylinders and a concrete frame. Experimental results have verified the effectiveness and the multi-functionality of the proposed smart aggregates. The multi-functional smart aggregates have the potential to be applied to the comprehensive monitoring of concrete structures from their earliest stages and throughout their lifetime.

(Some figures in this article are in colour only in the electronic version)

1. Introduction

Concrete structures are the most popular civil structures. Throughout the life cycle of a concrete structure, many important issues have to be addressed properly to ensure its safe operation.

During the construction phase or early age of a concrete structure, strength monitoring is vital to ensure the safe construction of a structure and to determine its readiness for service. The collapse of the Willow Island (West Virginia) cooling tower during its construction highlights the importance of early concrete strength monitoring. The primary cause of the collapse, which killed 51 workers, was insufficient strength

---

[3] Author to whom any correspondence should be addressed.

development of the concrete due to low temperature (mid-thirties Fahrenheit), a temperature at which a much longer time is required for the concrete to gain sufficient strength (Lew *et al* 1979, Feld and Carper 1997).

During the service life of a concrete structure, such as highway bridges or a bridge pier, it is important to detect vehicle–bridge collision and evaluate the damage as early as possible after the collision. Based on the impact level, appropriate actions, such as requesting further inspections or closing the operation of the structure, should be taken to prevent catastrophic consequences. The fatal 1993 Amtrak Mobile derailment accident, which was caused by a deformed rail resulting from barge impact on the bridge pier (NTSB 1994), speaks to the need for such an impact detection system, which would have saved 57 lives if installed. In a 2003 report by the Federal Highway Administration (FHWA), vehicle or ship impact with bridges is listed as potential terror attacks (FHWA 2003) on infrastructures. The Department of Homeland Security has identified (Tedesco 2006) that bridge impact is a major security and economic threat to America. The NTSB has recently (NTSB 2004) issued a recommendation stating that all bridges should be fitted with an impact warning system and sensors that detect the level of damage due to impact.

In addition to impact, many other factors, such as earthquakes or hurricanes, will cause damage to concrete structures. It is imperative to quickly assess the severity of the damage and health status of a structure, especially for an infrastructure, in real time or near-real time after such an event to provide vital information for decision-makers. It is desirable to have an automated and distributive system to perform the task of damage detection and health monitoring. In a recent runaway barge–bridge collision incident (Desmon and Linskey 2006), a key bridge north of Annapolis was closed for hours until a thorough inspection was completed. This incident highlights the need for such an automated system, which has the potential to greatly reduce the inspection time.

At present, there is no single transducer that can perform all these tasks at a low cost. This paper systematically presents *Smart Aggregate (SA) technology* that was recently developed by the authors. Smart aggregates are low cost piezoceramic-based multi-functional devices, which are capable of performing comprehensive monitoring of the concrete structures, including early-age strength monitoring (Gu *et al* 2006), impact detection and evaluation (Song *et al* 2007b), and structural health monitoring (Song *et al* 2007a). To monitor the early-age strength of concrete, one smart aggregate is used as an actuator to generate high frequency harmonic signals; the other smart aggregates are used as sensors. The harmonic amplitude is correlated with the compressive strength of early-age concrete by a fuzzy correlation system trained by experimental data. Experimental results show that the trained fuzzy correlation system can successfully predict the compressive strength on later occasions. For impact detection, the experimental results show that the peak value of the embedded piezoceramic signal is proportional to the impact force. For concrete structural health monitoring, a smart aggregate-based active sensing system is developed. In the

proposed active sensing system, one smart aggregate is used as an actuator to generate a sweep sine signal while the other smart aggregates are used as sensors to detect the sweep sine response. The propagation energy of the waves will be attenuated by cracks in the concrete structure. By analyzing the sensor signal, the health status of the concrete structure is evaluated. In the proposed health monitoring approach, wavelet packet analysis is used as a signal-processing tool. Based on the wavelet packet analysis results, a damage index is formed to evaluate the severity of the damage. To extract the time-history and location information of damage, two types of innovative damage index matrices are developed: a sensor-history damage index matrix and an actuator–sensor damage index matrix. Different types of concrete specimens, such as concrete bridge bent-caps and frames, have been utilized as testing objects. Experimental results have shown that the proposed structural health monitoring method is better than traditional methods with regards to detection of the existence and evaluation of crack severity. This paper also presents the results of using smart aggregates in comprehensive monitoring of a concrete frame structure based on their multi-functionalities. In summary, the multi-functional smart aggregates have the potential to be applied in the comprehensive monitoring of concrete structures from their earliest stages and throughout their lifetime.

2. Literature review

2.1. Review of early-age concrete strength monitoring

In the concrete structure industry, a destructive evaluation method is generally used, in which concrete cylinders are crushed, to directly obtain concrete strength information. This method is straightforward and reliable. However, this method is not suitable or convenient to monitor *in situ*, large-scale reinforced concrete (RC) structures. For non-destructive early-age performance monitoring of concrete, there are two major categories:

(1) *Hydration heat-based monitoring method.* By monitoring the heat generated during the hydration process, the early-age concrete performance can be continuously monitored by a thermocouple (Ayotte *et al* 1997) or an optical fiber (Lin *et al* 2004). Though this method is inexpensive, it is neither accurate nor reliable.
(2) *Ultrasonic-based monitoring method.* The velocity of an ultrasonic wave is closely related to the inner physical properties of the medium. Therefore, early-age concrete strength can be monitored by observing the propagation velocity of ultrasonic waves (Voigt *et al* 2005, Demirboga *et al* 2004, Krauss and Hariri 2001). A disadvantage of this method is its high cost and bulky equipment.

The harmonic magnitude-based method, which is used in this research, has not been found in the literature.

2.2. Review of impact detection

Impact detection can be classified into four major categories by the sensor types employed: (1) accelerometer-based impact
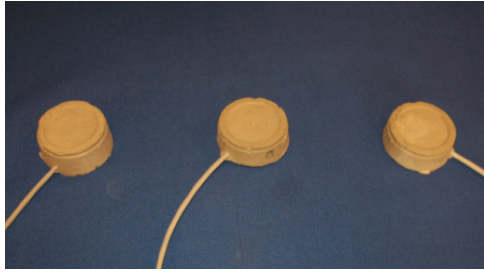
Figure 1. Three fabricated smart aggregates.

detection (Bernard *et al* 1988), (2) force sensor-based impact detection (Fujii and Fujimoto 1999), (3) piezoelectric-based detection (Staszewski *et al* 2000, Song *et al* 2007b) and (4) optical fiber-based impact detection (Yang and Han 2002). In general, the piezoelectric-based method is suitable for either surface mount or embedment, is low cost, and has a near-linear response. With piezoceramic-based SAs, piezoelectric-based impact detection methods will be used in this paper.

2.3. Review of health monitoring of concrete structures

Damage detection and failure analysis of concrete structures have been studied for many years (Otani and Sozen 1972, Abrams and Sozen 1979, Saiidi *et al* 1981, Kreger and Sozen 1983, Park *et al* 1985, Hassan and Sozen 1997, Wang and Wen 2000, Wen 2001, Nojavan and Yuan 2006). Various sensors and methods have been developed for damage detection and health monitoring. Fiber optical sensors (FOS), especially fiber Bragg grating (FBG) sensors, are now used for the health monitoring of various RC structures (Zhang *et al* 2006, Ren *et al* 2006, Lu and Xie 2006, Chen and Ansari 2000). However, FOSs are fragile and expensive, and offer only local measurements, which limit their applications. Piezoelectric-based approaches have provided an innovative approach for the structural health monitoring of civil structures with the advantages of structural simplicity, low cost, quick response and high reliability. In general, there are three major piezoelectric-based health monitoring approaches:

(1) *The impedance-based health monitoring approach* is a real-time, qualitative damage detection method (Hey *et al* 2006, Naidu and Bhalla 2003, Tseng and Wang 2004). The operating principle is based on the electromechanical coupling property of piezoelectric materials. The impedance-based approach has been applied to the health monitoring of trusses (Sun *et al* 1995), aluminum specimens (Tseng and Naidu 2002), RC bridges (Soh *et al* 2000), RC specimens (Bhalla and Soh 2004, Park *et al* 2006), RC shear walls (Zhao and Li 2006) and composite reinforced concrete/masonry walls (Raju *et al* 1999). Normally, impedance-based approaches require a sampling rate of several hundred kHz, which is beyond the capacity of most microprocessors and wireless transmitters and may not be suitable for distributive or wireless deployment.
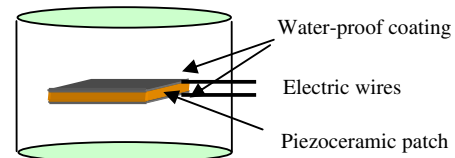
Figure 2. Illustration of a smart aggregate.

(2) *The vibration-characteristic approach* utilizes piezoelectric actuators to generate certain waves, which propagate within the structure, and compares the structural vibration-characteristic parameters (modal shape, model frequency) (Okafor *et al* 1996), vibration-characteristic response curves (sweep sine response (Song *et al* 2007a)) or transfer function (Saafi and Sayyah 2001) with those of the healthy state to detect damage. Delamination between a reinforcing bar and concrete has also been studied using this approach (Miller *et al* 2002, Na and Kund 2003). This approach works with a wide spectrum of excitation frequencies, including several hundred Hz to several kHz, and will be adopted in this paper with the help of innovative damage index matrices, to be defined later.

(3) *Lamb wave-based health monitoring approach* is used with PZT (an acronym for lead zirconate titanate, a commonly used piezoceramic material due to its strong piezoelectricity) patches either surface bonded to, (Lim *et al* 2006) or embedded in (Song *et al* 2007a), the structure to detect structural damage by generating a Lamb wave and monitoring its reflections. However, this approach is not suitable for concrete structures, which have complex geometries and are usually not thin-shell structures.

3. Piezoelectric-based smart aggregate

In this paper, the *smart aggregates* (SAs) shown in figure 1 are formed by embedding a waterproof piezoelectric patch with lead wires into a small concrete block before casting the smart aggregate into a larger concrete structure. Piezoelectric transducers are very fragile and can be easily damaged by the vibrator during the casting of concrete structures. In order to protect the fragile piezoelectric transducer, the piezoelectric patch is first applied with an insulation coating to prevent water and moisture damage and then embedded into a small concrete block to form a smart aggregate as shown in figure 2. The smart aggregate can then be embedded at the desired position in the concrete structure before casting, eliminating the risk of damaging the transducer during the vibrating process. The materials to build the small concrete block have the same mixture of cement, sand and water as the host concrete structure. In this way, the smart aggregates will have almost no effect in changing the material properties and the structural properties of the host concrete structures.

The piezoelectric material will generate an electric charge when it is subjected to a stress or strain (the direct piezoelectric effect); the piezoelectric material will also produce a stress or strain when an electric field is applied to a piezoelectric

material in its poled direction (the converse piezoelectric effect). Due to this special piezoelectric property, piezoelectric material can be utilized as both an actuator and a sensor. This property enables the multi-functionality of the smart aggregates. Additionally, piezoelectric materials have the advantages of being lightweight, low cost, fast responding and having solid-state actuation, making them ideal for comprehensive monitoring of concrete structures.

4. Principle of multi-functionality of smart aggregate

For the construction of a concrete structure, early-age performance monitoring is an important process. After the concrete is cured and the strength fully developed, it is also important to conduct structural health monitoring to detect the existence and development of cracks. For *in situ* concrete structures, such as highway bridge girders, collision accidents with overheight (exceeding the maximum vertical clearance) trucks often happen. It is important to detect the occurrence of the impact, to evaluate the impact force and to investigate the damage of the concrete structure. For safety and maintenance purposes, the health status of the concrete structure should be monitored. In this paper, smart aggregates are utilized for the early-age strength monitoring of concrete, impact detection and structural health monitoring.

4.1. Principle of early-age concrete strength monitoring

4.1.1. Motivation. The evaluation of concrete during the curing process or at an early age is a major concern for the construction of concrete structures. There are two major categories of non-destructive evaluation methods used for the early-age performance monitoring of concrete: hydration heat-based monitoring methods (Lin *et al* 2004) and ultrasonic technology-based monitoring methods (Demirboga *et al* 2004). In this research, smart aggregates are embedded into concrete specimens for early-age strength monitoring by using high frequency harmonic excitation.

4.1.2. Principle. The wave propagation of stress waves in concrete cylinders can be viewed as one-dimensional longitudinal wave propagation. The wave equation (Achenbach 1973) can be written as

$$\frac{\partial^2 u}{\partial x^2} = \frac{1}{c_b^2}\frac{\partial^2 u}{\partial t^2}(c_b^2 = E/\rho), \tag{1}$$

where u is the displacement of an element, E is the Young's modulus and ρ is the density of the material.

The average power, p, of the harmonic response over a period can be expressed as

$$p = EA^2\omega^2/2c_b = \sqrt{E\rho}A^2\omega^2/2, \tag{2}$$

where A is the harmonic amplitude and ω is the circular, or angular, frequency.

Equation (2) can be rewritten as

$$A = \left(\frac{1}{\omega}\right)\left(\frac{4p^2}{E\rho}\right)^{\frac{1}{4}}. \tag{3}$$

As shown in equation (3), the harmonic amplitude is affected by the Young's modulus, E, of the medium. During the early-age development of concrete, the Young's modulus, E, increases as the concrete stiffens and gains strength during the hydration process. Consequently, the harmonic amplitude will decrease with the increase of the Young's modulus, E. Moreover, the Young's modulus, E, is the major affecting factor in determining concrete strength. Therefore, the harmonic amplitude is correlated with the concrete strength through the status of the Young's modulus. By observing the change of harmonic amplitude, the strength development of concrete specimens can be monitored and evaluated.

4.2. Principle of impact detection and evaluation

4.2.1. Motivation. One of the most common types of damage in existing highway bridges is the damage at the bottom corners or edges of the reinforced concrete beams or box girders induced by impact with trucks exceeding the allowable height clearance of the bridges. The development of an overheight collision detection and evaluation system is of pressing importance in order to identify the occurrence and magnitude of such impact damage and, thus, ensure the continued safety of the bridge structure. In this section, piezoceramic-based smart aggregates are used to detect impact caused by an overheight vehicle and to trigger a camera to capture and record the offending vehicle. Additionally, the smart aggregate can evaluate the damage caused by the impact and perform structural health monitoring.

4.2.2. Principle. At present, the most suitable and popular piezoelectric ceramic materials are lead zirconate titanates (PZTs). In the proposed impact detection and evaluation system, PZT patches are used as transducers embedded into the concrete before casting. The open-circuit voltage yielded by the PZT transducer when compressed with force F is given by

$$V = \frac{g_{33}Ft}{A}, \tag{4}$$

where A is the area of the transducer, t is the thickness of the PZT transducer and g_{33} is the piezoelectric voltage constant. The piezoelectric voltage constant is defined as the electric field generated in a material per unit mechanical stress applied to it. The first subscript refers to the direction of the electric field generated in the material or the applied electric displacement; the second refers to the direction of the applied stress or the direction of the induced strain. From equation (4), the open-circuit voltage yielded by the PZT transducer is proportional to the compressed force and can be utilized to evaluate the impact force.

4.3. Principle of structural health monitoring

4.3.1. Motivation. In recent years, there has been an increasing demand for the structural health monitoring of large-scale structures to reduce maintenance costs and to enhance safety. Traditional health monitoring methods (x-ray, C-scan, etc) are expensive and sometimes ineffective for large-scale structures with limited or no accessibility. Piezoelectric
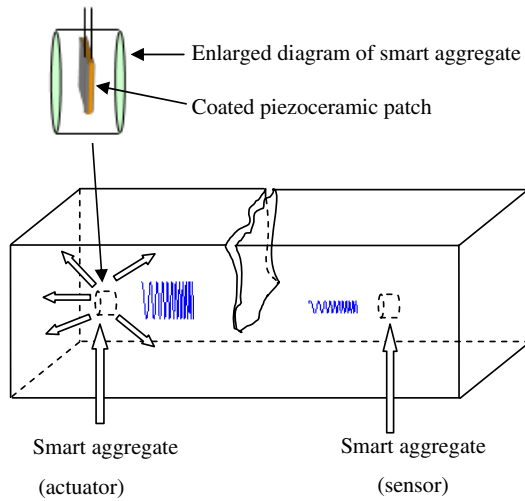
Figure 3. Block diagram of a piezoelectric-based active sensing system.

transducers have emerged as new tools for the health monitoring of large-sized structures due to their advantages of active sensing, low cost, quick response, availability in different shapes and simplicity of implementation.

4.3.2. Principle. In this research, a smart aggregate-based active sensing system, as shown in figure 3, was developed for the health monitoring of large-scale concrete structures. The piezoelectric transducer in one smart aggregate is used as an actuator to send excitation waves. The piezoelectric transducers in the other, distributed smart aggregates are used as sensors. The crack or damage inside the concrete structure acts as a stress relief in the wave propagation path. The amplitude of the wave and the transmission energy will decrease due to the existence of a crack. The drop value of the transmission energy will be correlated with the degree of the damage inside.

Wavelet packet analysis is used as a signal-processing tool to analyze the sensor signal of the embedded PZT patches in the concrete structure. A wavelet is a waveform of effectively limited duration that has an average value of zero. In wavelet analysis, a signal is split into an approximation (low frequency information) and a detail (high frequency information). The approximation is then itself split into a second-level approximation and detail, and the process is repeated. In wavelet packet analysis, the details as well as the approximations can be split. The advantage of wavelet packet analysis is that it enables the inspection of relatively narrow frequency bands over a relatively short time window.

The sensor signal S is decomposed by an n-level wavelet packet decomposition into 2^n signal sets $\{X_1, X_2, \ldots, X_{2^n}\}$. $E_{i,j}$ is the energy of the decomposed signal, where i is the time index and j is the frequency band ($j = 1 \ldots 2^n$). X_j can be expressed as

$$X_j = [x_{j,1} x_{j,2}, \ldots, x_{j,m}], \tag{5}$$

where m is the amount of sampling data. Additionally, the energy of the decomposed signal is defined as

$$E_{i,j} = \|X_j\|_2^2 = x_{j,1}^2 + x_{j,2}^2 + \cdots + x_{j,m}^2. \tag{6}$$

The energy vector at time index i is defined as

$$E_i = [E_{i,1}, E_{i,2}, \ldots, E_{i,2^n}]. \tag{7}$$

Various kinds of damage indices have been developed for health monitoring of civil structures in recent years. Root-mean-square deviation (RMSD) is a commonly used damage index to compare the difference between the signatures of healthy and damaged states (Soh *et al* 2000, Tseng and Naidu 2002). In the proposed approach, the damage index is formed by calculating the RMSD between the energy vectors of the healthy state and the damaged state. The energy vector for healthy data is $E_h = [E_{h,1}, E_{h,2}, \ldots, E_{h,2^n}]$. The energy vector E_i for the damaged state at time index i is defined as $E_i = [E_{i,1}, E_{i,2}, \ldots, E_{i,2^n}]$. The damage index at time i is defined as

$$I = \sqrt{\sum_{j=1}^{2^n} (E_{i,j} - E_{h,j})^2 \Big/ \sum_{j=1}^{2^n} E_{h,j}^2}. \tag{8}$$

The proposed damage index represents the transmission energy loss portion caused by structural damage. When the damage index is close to 0, the concrete structure is in a healthy state. When the damage index is larger than a certain threshold value, damage has begun to appear in the concrete structure. In this case, the greater the index, the more serious the damage.

To demonstrate the health status at different locations of the concrete structure, two types of damage index matrices are defined, a sensor-history damage index matrix and an actuator–sensor damage index matrix.

(1) *A sensor-history damage index matrix (SHDIM)* $M_{m \times n}$ is defined as

$$M_{m \times n} = \big[I_{i,j}\big]_{m \times n} \quad (i = 1, \ldots m \text{ and } j = 1, \ldots, n), \tag{9}$$

where the matrix element at the ith row and the jth column, $I_{i,j}$, is the damage index of the ith smart aggregate at the time of the jth test (i.e. i is the sensor index, j is the time index); m is the total number of smart aggregates and n is the total number of tests. The damage status at different locations of the concrete specimen at different test times can be described by a three-dimensional damage index matrix plot. The SHDIM is useful in monitoring the damage evolution process to predict the failure of a structure.

(2) *An actuator–sensor damage index matrix (ASDIM)* $D_{m \times k}$ is defined as

$$D_{m \times k} = \big[I_{i,j}\big] \quad (i = 1, \ldots, m \text{ and } j = 1, \ldots, k), \tag{10}$$

where the element at the ith row and the jth column in the matrix, $I_{i,j}$, is the damage index in the case that the ith smart aggregate is used as a sensor and the jth smart aggregate is used as an actuator, m is the total number of smart aggregates as sensors and k is the total number of smart aggregates as actuators. The actuator–sensor pair damage index shows the damage status between different actuator–sensor pairs. The ASDIM is useful in extracting damage location information.

Table 1. Compositional details of the concrete tested.

Component	Quantity (lb/cubic yard) (weight of component, lb/ volume of concrete, 1 cu.yd)	Description
Cement	580	Type I-Portland cement
Sand	1535	Standard sand
Coarse aggregate	1697	1/2 inch size angular limestone
Water	355	Potable water

Table 2. Details for each test during the loading process.

Test no.	Description	Test no.	Description
1	Health status	8	Displacement = 1.9 in
2	Load = 4.41 kips	9	Displacement = 2.5 in
3	Load = 6.61 kips	10	Displacement = 3 in
4	Load = 8.82 kips	11	Displacement = 3 in
5	Load = 11.02 kips	12	Displacement = 3.5 in
6	Displacement control starts Displacement = 1.6 inches	13	Displacement = 4 in
7	Displacement = 1.9 inches	14	Unload

5. Experimental programs

Different types of concrete specimens are used as testing objects. Concrete cylinders are used as test objects for early-age strength monitoring. A concrete beam is used as a test object for impact detection and evaluation. Two concrete bent-caps are used as test objects for structural health monitoring. A two-story concrete frame is used as a test object for comprehensive monitoring, which includes early-age strength monitoring, impact detection and structural health monitoring together.

5.1. Experimental program of early-age strength monitoring (Gu et al 2006)

5.1.1. Experimental set-up. In this research, 34 concrete cylinder specimens with 6 inch diameter and 12 inch height were fabricated and tested for compressive strength in accordance with the ASTM C39/39M-2003 specification. Among these cylinder specimens, three concrete cylinders were instrumented with smart aggregates and are referred to as specimens I, II and III. The details of composition of the concrete tested are presented in table 1. The water/cement ratio by weight of the concrete was 0.61. The experimental set-up for the early-age strength monitoring of the concrete is shown in figure 4. The harmonic signal is generated by an Agilent 33120A function/arbitrary waveform generator and amplified by a Quickpack power amplifier (Model EL1224) before exciting the piezoelectric actuator embedded in the concrete. The harmonic response signal of the piezoelectric sensor is recorded through a LeCroy digital oscilloscope (Model Waverunner LT342).

5.1.2. Experimental results. Compressive tests using a universal compression testing machine were conducted to obtain the strength values of the concrete specimens. In each compressive test, three concrete cylinders are crushed at the same time. The compressive strength is recorded as the average
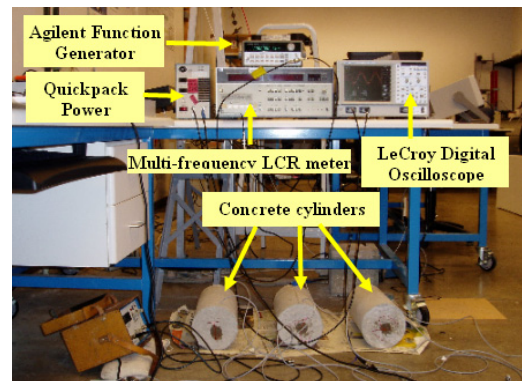
Figure 4. Experimental set-up for early-age strength monitoring of concrete cylinder specimens.

value of the compressive strength for the three tested concrete cylinders. The compressive strength versus age (day) plot is shown in figure 5. It is clear that the compressive strength increased at a fast rate for the first 7 days. After the 7th day, the strength developed at a decreasing rate.

For the smart aggregate-based strength test, three concrete cylinders instrumented with smart aggregates were excited by different high frequency harmonic signals. From the harmonic amplitude versus age (day) plot with different harmonic frequencies excitation, as shown in figure 6, it is clear that the harmonic amplitude dropped at a fast rate for the first 7 days, and after the 7th day, the amplitude dropped at a decreasing rate.

Concrete is heterogeneous and anisotropic. The correlation between the harmonic amplitude and the compressive strength of concrete is highly nonlinear and complex, which makes it extremely difficult to develop a mathematical model. In this paper, a fuzzy correlation system is trained to correlate the harmonic amplitude with the strength of concrete by using the batch least squares algorithm. The input variable of the proposed fuzzy correlation system is the amplitude of the har-
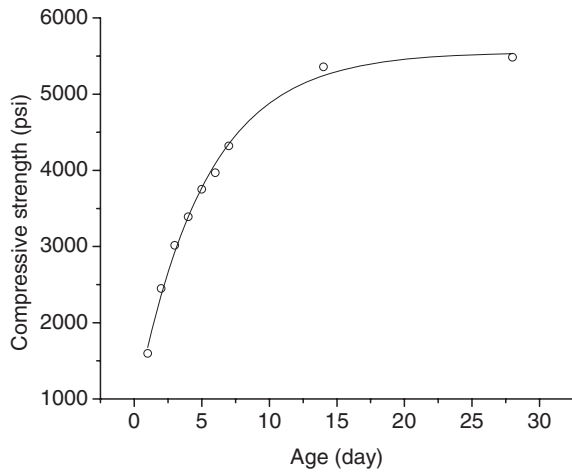
Figure 5. Compressive strength versus age.
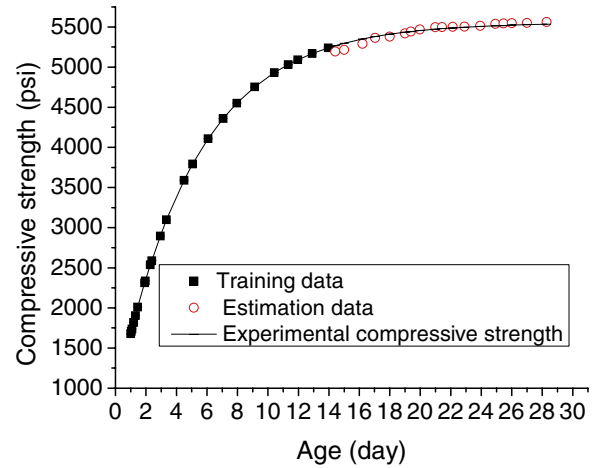
Figure 7. Experimental compressive strength and estimated compressive strength.
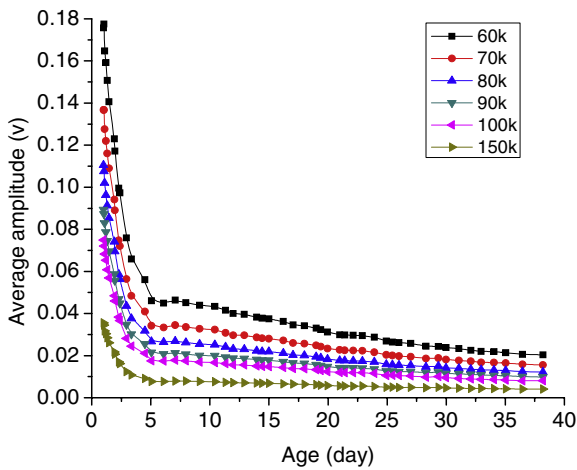
Figure 6. Amplitudes of different harmonic excitation.

monic response from the piezoelectric sensor. The output variable of the fuzzy correlation system is the concrete compressive strength. Four linguistic variables (small, less medium, medium, large) are defined to represent the input domain and output domain with their membership values lying between 0 and 1. The Gaussian membership function is a commonly used membership function and it is applied to represent the different linguistic variables for input and output domain in this paper. Gaussian functions are realized by

$$\mu(x) = e^{\frac{(x-a)^2}{\sigma^2}}, \qquad (11)$$

where μ is the membership function value, x is the input variable, a is the center of the membership function and σ is the width of the membership function. The fuzzy inference rules are defined as:

Rule 1: IF the harmonic amplitude is small, THEN the compressive strength is large.

Rule 2: IF the harmonic amplitude is less medium, THEN the compressive strength is medium.

Rule 3: IF the harmonic amplitude is medium, THEN the compressive strength is less medium.

Rule 4: IF the harmonic amplitude is large, THEN the compressive strength is small.

The center average defuzzification method is used in the proposed approach. The output y^* of the fuzzy correlation system is defined as

$$y^* = \sum_{l=1}^{4} \bar{y}^l \mu_l(x) \bigg/ \sum_{l=1}^{4} \mu_l(x), \qquad (12)$$

where $\bar{y}^l$ is the center of the lth output membership function.

Amplitude–strength mapping data of the 60 kHz harmonic excitation from the first 14 days are used to train a fuzzy correlation system which relates the harmonic amplitude to the compressive strength.

To verify the effectiveness of the trained fuzzy correlation system, the harmonic amplitude data from the 14th to 28th day are used as input data to the trained fuzzy correlation system to generate the estimated value for the compressive strength of concrete from 14 to 28 days. The harmonic amplitude–concrete strength mapping data from the 14th to 28th day are not included in the training set. Therefore, it is valid to use them to verify the effectiveness of the trained fuzzy correlation system. The experimental results show that the compressive concrete strength estimated by the fuzzy correlation system from the 14th to 28th day matches the experimental compressive strength, as shown in figure 7. The presented experimental results are for the initial stage of this research to verify the concept and principle of using smart aggregate sensor data to monitor and predict the concrete strength. In future research, large quantities of concrete specimens will be used to obtain the nonlinear relationship to predict the concrete strength development as soon as the smart aggregates are embedded into the concrete structures based on the sensor output voltage.

5.2. Experimental program of impact detection and evaluation (Song et al 2007b)

5.2.1. Experimental set-up. In this research, a smart aggregate-based impact detection and evaluation system is
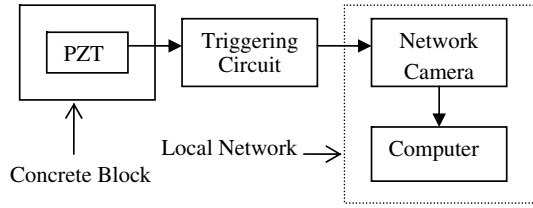
Figure 8. Block diagram of impact detection and the image capturing system.
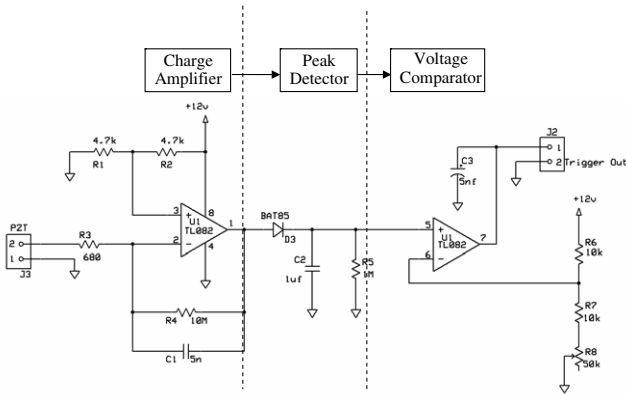
Figure 9. Triggering circuit block diagram and schematic.

Figure 10. PZT sensor signal and output signal from the triggering circuit during impact.

presented. An overheight impact detection and evaluation system based on piezoelectric materials is presented. The proposed method can be divided into two sections: (a) an overheight impact detection and image capturing system and (b) an impact evaluation system.

A concrete beam 101.6 mm × 914.4 mm × 19 mm (4 in × 36 in × 0.75 in) was fabricated as a test object. Three piezoelectric patches (PZT1, PZT2 and PZT3) coated with a waterproof coating are used. The size of each piezoelectric patch is 8 mm × 8 mm × 0.267 mm and the piezoelectric voltage constant, g_{33}, is 24.0×10^{-3} V mN^{-1}. To detect the impact, a circuit was designed to read the PZT signal and output a trigger or activating signal to an image capturing system at the moment of impact, as shown in figure 8. The triggering circuit block diagram and schematic are illustrated in figure 9.

The internal capacitance of PZT sensors combined with an external resistive load is equivalent to a high pass filter. To avoid reducing the signal strength at low frequencies, a charge amplifier design was used. The amplifier produces a voltage proportional to the input charge; thus, small changes in the input capacitance will not affect the output amplitude. The following equation describes the transfer function of the amplifier:

$$H(s) = -\frac{\tau_l s}{(\tau_h \tau_l) s^2 + (C_{PZT} R_3 + C_1 R_4) s + 1}, \qquad (13)$$

where τ_h and τ_l respectively represent the higher and lower time constants that define the bandwidth of the amplifier. In the first case, $\tau_h = R_3 C_1 = 3.4$ μs or $\frac{1}{\tau_h} \approx 294$ kHz, and in the second case $\tau_l = R_4 C_{PZT} = 50$ ms, or $\frac{1}{\tau_l} = 20$ Hz.

After amplifying the piezoelectric signal, the circuit identifies the highest voltage reached using a peak detector

composed of a simple diode–capacitor combination. The last block in the triggering circuit compares the peak detector voltage with a preset voltage reference. The output will be at a high voltage when an impact is detected and it will stay high for

$$t = -R_5 C_2 \ln\left(\frac{V_{\text{ref}}}{V_{\text{pk}}}\right), \qquad (14)$$

where V_{ref} is the preset voltage reference, and V_{pk} and the product $R_5 C_2$ are, respectively, the voltage detected and the time constant of the peak detector. The preset voltage reference should be used to change the impact sensibility of the circuit.

To actually capture the picture of the offending vehicle, the output of the triggering circuit was directly connected to the network camera trigger input. Through an internet-based interface, the camera was set up to connect to a local computer and save a picture of the impact when a rise in voltage is detected at the trigger input. To accomplish the transfer of images, a local network was set up using a router and an FTP server on the local computer. To simplify the experimental set-up, administrator privileges were granted to the FTP client that will eventually connect to save the pictures.

5.2.2. Experimental results. After setting up the experiment, a radio-controlled truck was collided several times into the concrete block. The signal generated by the piezoelectric sensor and the output trigger was recorded using Labview. During pre-testing, the radio-controlled truck did not create a strong enough impact. To detect the impact, the sensitivity of the circuit, or preset value, was adjusted. Through the following experiments, the preset voltage reference was experimentally found to be around 6 V for the specific PZT sensor and background noise of the lab. The specific value allowed the circuit to reject noise and random vibrations detected by the sensor. Preset values may change depending on the type of sensor, size of concrete block and minimum desired impact to be detected. In the first impact after the pre-testing period, the circuit captured and processed the signal correctly. At the same time, the network camera took a picture of the ongoing impact. Figure 10 shows the signal detected by the PZT sensor and the output trigger signal from the circuit.
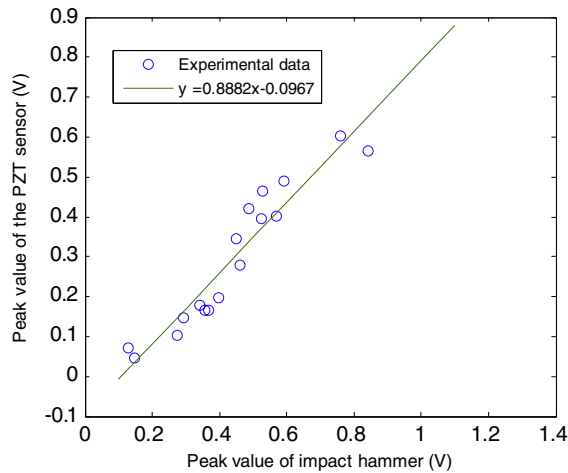
Figure 11. PZT impact peak voltage versus the peak value of the hammer.

For impact evaluation testing, a modally Tuned Impact Hammer (model no. 086C03, PCB Inc.), with an operating sensitivity of 2.25 mv N^{-1} and mass of 0.16 kg, was used. A LeCroy Waverunner digital oscilloscope (model no. LT 342) was used to record the impact signal and the sensor signal from the embedded piezoelectric transducer. When the hammer impacted the concrete specimen, the impact impulse signal was obtained from a PZT transducer embedded inside the hammer. The output voltage from the impact hammer is proportional to the impact force. From the impact hammer experimental results shown in figure 11, it can be seen that the peak value of the impact sensor is proportional to the peak value of the impact hammer. The peak value of the impact sensor can be used to estimate the impact force peak value.

5.3. Experimental program of structural health monitoring (Song et al 2007a)

5.3.1. Experimental set-up. The test specimen as shown in figure 12 is a specially designed bent-cap with a working capacity of 1050 kips located in the Structural Research Laboratory at the University of Houston. During the experiment, the load of the four hydraulic actuators is gradually increased until the concrete structure fails. As the bent-cap is loaded, cracks appear inside the concrete structure and gradually the concrete bent-cap becomes severely damaged. Two full-sized, reinforced concrete bridge bent-caps are used as testing objects. In specimen W1, the first concrete bridge bent-cap, four smart aggregates were placed in planar positions in one end of the concrete bent-cap. In specimen W2, the second concrete bridge bent-cap, ten smart aggregates were placed in spatial positions in the concrete bent-cap as shown in figure 13. The acoustic emission (AE) Kaiser effect was first investigated by Joseph Kaiser in 1950 to describe the phenomenon that acoustic emission signals are not produced until the previous maximum load is exceeded. In the test procedure, the load to fail the concrete structure is continually increasing until structural failure. The load used is not a cyclic load; therefore the acoustic emission (AE) Kaiser effect will not affect the experimental results.
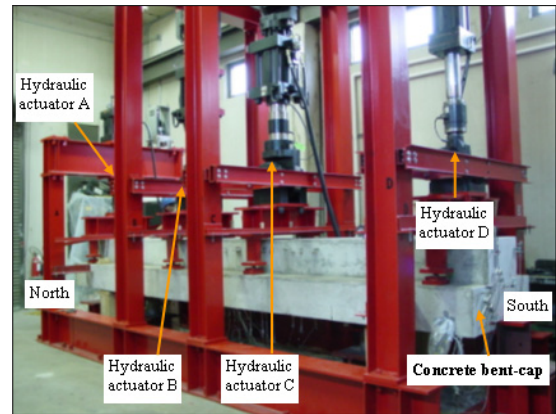
Figure 12. Experimental set-up for structural health monitoring.
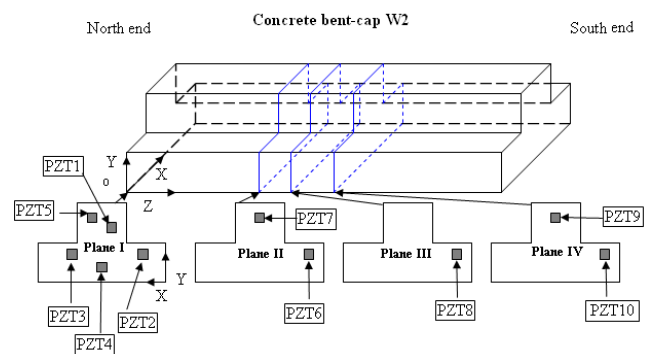
Figure 13. Location of smart aggregates in specimen W2.

5.3.2. Experimental results. During the experiment, the load was gradually increased to crack the concrete specimen to a final failure. To measure the crack width, a microscope was used. From the experimental results of both specimens, as shown in figures 14 and 15, the damage index correlates well with the increasing trend of the loading curve. The experimental results prove that the damage index defined above can represent the severity and trend of the damage inside a concrete bent-cap. From the damage index curve of specimen W1, as shown in figure 14, the damage index is close to the critical value when the load is around 40 kips, the load value at which, from the LVDT and MS results of W1 as shown in figure 16, the crack width just begins to increase on the surface. From the experimental results of the second specimen W2, as shown in figure 15, the damage index reaches a critical point around 74 kips, the same load value at which the crack width on the surface has just begun to increase as shown in figure 17. These results indicate that severe cracks appeared before the crack width begins to increase on the surface. For both specimens, the critical points (a precautionary point to predict the structural failure) in the proposed method are ahead of the critical point deduced from LVDT and microscope results for both concrete bent-caps. This implies that the smart aggregate-based method is more sensitive than traditional health monitoring methods using LVDTs and microscopes. Due to its sensitivity, the proposed method can predict the structural failure before the structure
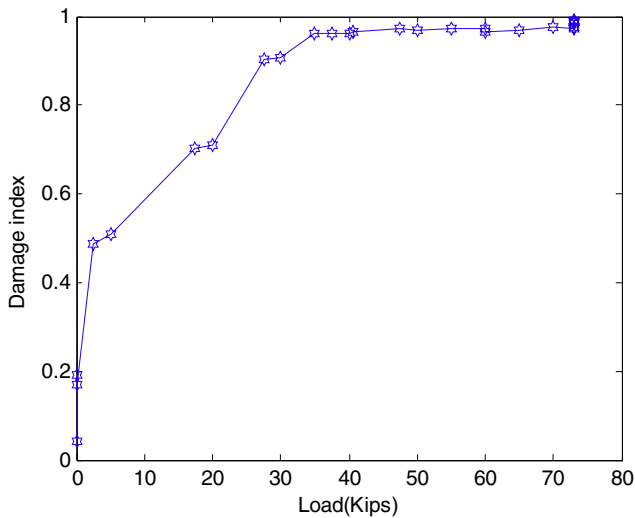
Figure 14. Damage index versus the load curve for specimen W1 of PZT2 with PZT1 as an actuator.
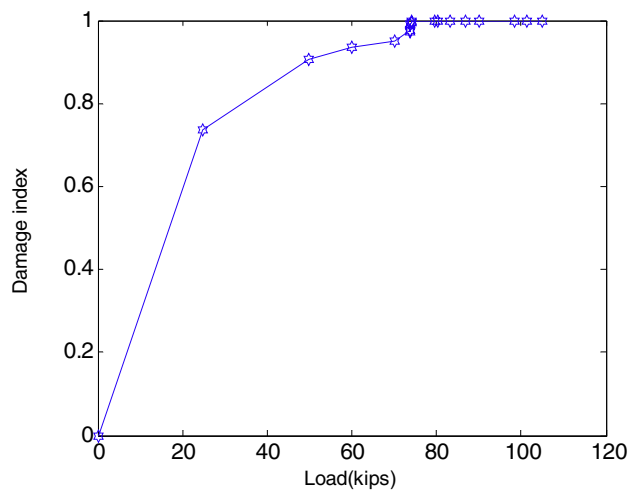
Figure 15. Damage index versus the load curve for specimen W2 of PZT2 with PZT3 as an actuator.

fails. The proposed method has the potential to be applied to *in situ* health monitoring of large-scale, reinforced concrete structures at an economical cost without using additional bulky equipment.

For the overheight vehicle collision detection system described in the previous section, a destructive test, via impacting a scaled-down concrete beam, was conducted. The proposed structural health monitoring method described in this section was applied to evaluate the damage after the impact. During this test, the concrete specimen was first impacted repeatedly by an impact hammer. Then, a 28 g ball and a 242 g ball were dropped freely to impact the concrete specimen repeatedly until it was damaged to a severe state. From the damage index history shown in figure 18, it can be seen that, during the impact tests, the damage index increased, indicating that the damage was growing with the repeated impact.

The first cracking noise is a predictive signal that the damage of the concrete structure starts. Capturing such
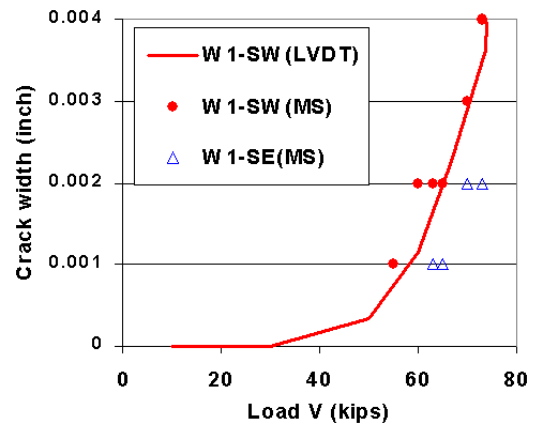
Figure 16. Crack width measured by a microscope and LVDT for the first specimen, W1.
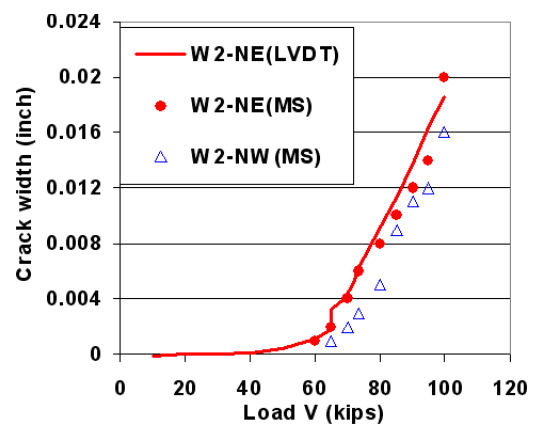
Figure 17. Crack width measured by a microscope and LVDT for the second specimen, W2.
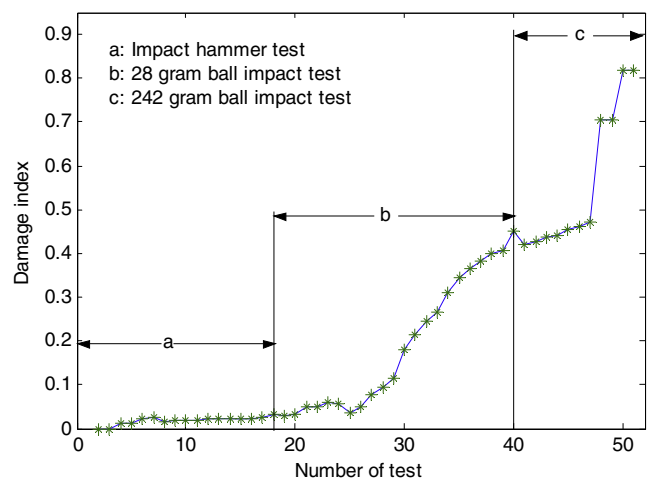
Figure 18. Damage index used during impact tests.

a critical moment is important for the structural health monitoring of concrete structures. The smart aggregate is also able to capture the moment of concrete cracking. By setting the oscilloscope in trigger mode to look for the sensor signal from the smart aggregate, the crack sound is captured, as shown in
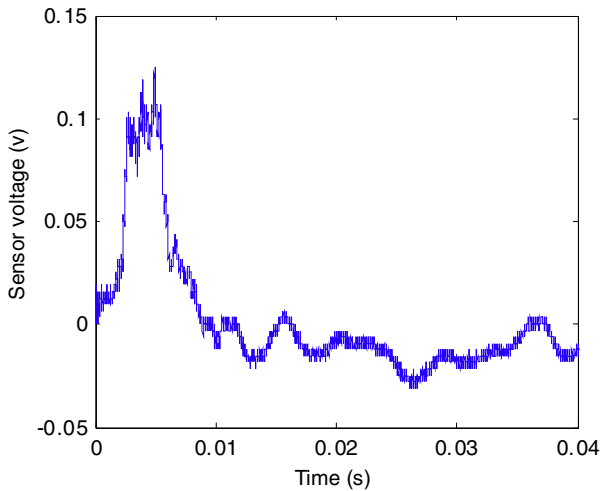
Figure 19. Cracking noise data captured by the smart aggregate at the moment of cracking.

figure 19, when a concrete specimen was gradually loaded to crack.

5.4. Experimental program for comprehensive monitoring

5.4.1. Experimental set-up. A two-story concrete frame instrumented with piezoceramic-based smart aggregates, as shown in figures 20 and 21, was fabricated as the object for comprehensive tests, including early-age strength monitoring, impact detection and structural health monitoring. Two hydraulic actuators were installed at right corners of the concrete frame to apply load to the frame structure and conduct the so-called 'push-over' test. The load was increasingly applied to the structure until failure. LVDTs were also installed to measure the displacement at different locations of the concrete frame.

5.4.2. Experimental results. The concrete strength of the concrete frame was monitored at its early age. After the concrete strength was fully developed, impact tests and structural health monitoring tests were performed on the concrete frame. Experimental results demonstrate the effectiveness and multi-functionality of the proposed smart aggregates.

(a) *Experimental results of early-age concrete strength monitoring.* As a reference, 36 concrete cylinders, 4 in diameter and 8 in height, were fabricated to help experimentally obtain the early-age concrete compressive strength as shown in figure 22. The concrete cylinder specimens were fabricated using the same concrete composition used to fabricate the 2-story concrete frame. Among the concrete cylinders, three of them were instrumented with piezoelectric-based smart aggregates to monitor the early-age concrete strength. Based on the experimental data of the compressive concrete strength, a compressive strength curve was plotted versus the age in days as shown in figure 23. The experimental data shows the compressive concrete strength increases quickly in the first week and continues to increase at a decaying rate for the remaining days.
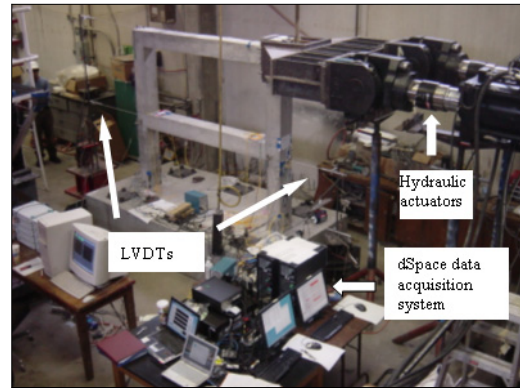
Figure 20. Concrete frame for the comprehensive performance evaluation test.
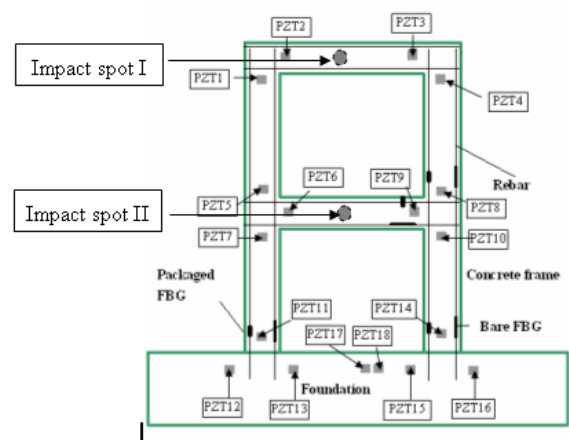
Figure 21. Locations of the smart aggregates.

The smart aggregate-based active sensing system is used to monitor the concrete strength. For comparison purposes, the harmonic response amplitudes are normalized to have the maximum value of 1. From the comparison of the average normalized harmonic amplitude in the concrete frame with that in the concrete cylinders shown in figure 24, it can be seen that the harmonic amplitude of the smart aggregates in both the concrete frame and the concrete cylinder share a similar development trend.

A fuzzy correlation system was trained based on the experimental data of the first 12 days' harmonic amplitude–compressive strength data pairs of the concrete cylinder specimens by using the batch least square algorithm. Five linguistic variables (smaller, small, medium, large, larger) are defined to represent the input domain and output domain with their membership values between 0 and 1, as shown in figures 25 and 26. Fuzzy inference rules are defined according to the experience that harmonic amplitude decreases as the concrete strength increases in the early age. The center average defuzzification method is used in the proposed fuzzy correlation system. The center values of the output membership function are identified by the batch least squares algorithm based on the training data. From the comparison of the output of the fuzzy correlation system with the

11
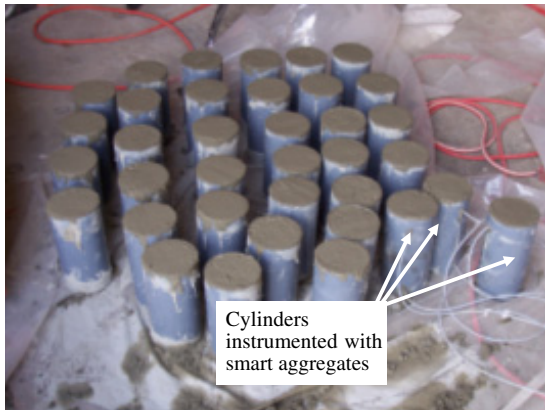
Figure 22. Concrete cylinders fabricated for the concrete strength test.

Figure 24. Comparison of the average harmonic amplitude in the concrete frame with harmonic amplitude in concrete cylinders.

Figure 23. Compressive strength versus age of the concrete.
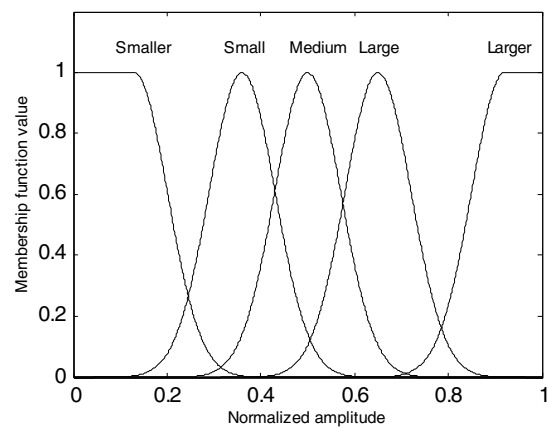
Figure 25. Membership functions of the input variable (harmonic amplitude).

experimental data as shown in figure 27, it can be seen that the output of the fuzzy correlation system is very close to the experimental training data. This means the input–output mapping of the trained fuzzy correlation system matches with the input–output mapping of the training data. The trained fuzzy system is used to estimate compressive strength of the concrete specimen at early age.

The estimated compressive concrete strength from the 12th to 28th day estimated by the fuzzy correlation system is shown in figure 28. The harmonic amplitude of the smart aggregate sensor from both cylinder and frame are used to predict the concrete strength from the 12th to 28th day. From the experimental results, it can be seen that the predicted 12th to 28th day concrete strength using the cylinder data matches the experimental data of the concrete strength. By using concrete frame experimental data as the input for the fuzzy correlation system, the predicted compressive strength also matches the experimental data well, although the fuzzy correlation system is trained by the experimental data from concrete cylinders. This means that the correlation system trained by the experimental cylinder data can be used for the concrete strength monitoring of the concrete frame.

(b) *Experimental results of impact detection and evaluation.* During the impact detection test, the concrete

frame is impacted by a hammer at impact spots I and II, as shown in figure 21. From the time responses of the smart aggregate sensors shown in figures 29 and 30, it can be seen that the impulse response is captured by all distributed smart aggregates when the concrete frame is impacted either on spot I or spot II. When the concrete frame is impacted on spot I, the sensor signal of PZT2 has greater amplitude compared to the other sensors. When the concrete frame is impacted on impact spot II, the sensor signal of PZT5 has greater amplitude compared with other sensors. The energy of the ith sensor signal E_i is defined as

$$E_i = \int u^2 \, \mathrm{d}t, \qquad (15)$$

where u is the sensor voltage and t is the time. From the sensor energy plot shown in figure 31, it can be seen that, when the concrete frame is impacted on spot I, the sensor signal of PZT2 has greater sensor energy compared to other sensors. This is because PZT2 is the closest to impact spot I compared to the other sensors. When the concrete frame is impacted on spot II, the sensor signal of PZT5 has greater sensor energy compared to the other sensors. This is because PZT5 is closer to impact spot II compared to the other smart aggregates.
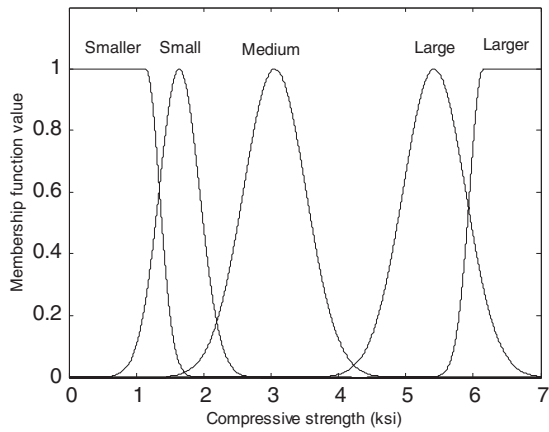
Figure 26. Membership functions of the output variable (compressive strength).
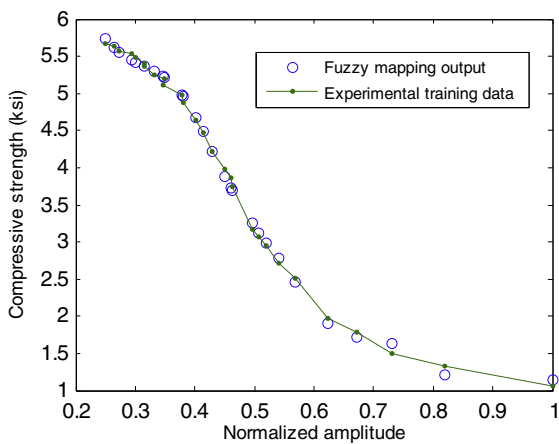
Figure 27. Comparison of the fuzzy mapping output with the experimental training data.
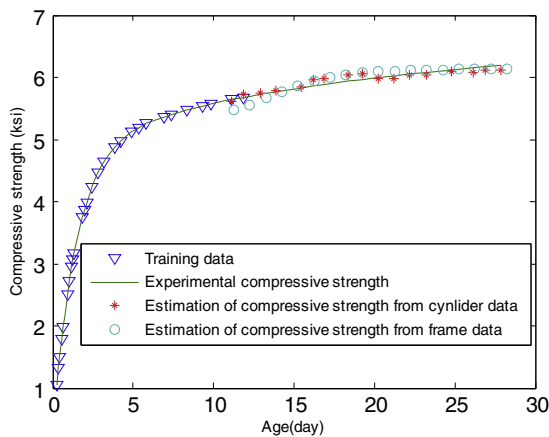
Figure 28. Comparison of the experimental compressive strength with an estimation of the compressive strength using the proposed correlation system.

Figure 29. Impulse responses captured by smart aggregate sensors when the concrete frame is impacted at impact spot I.
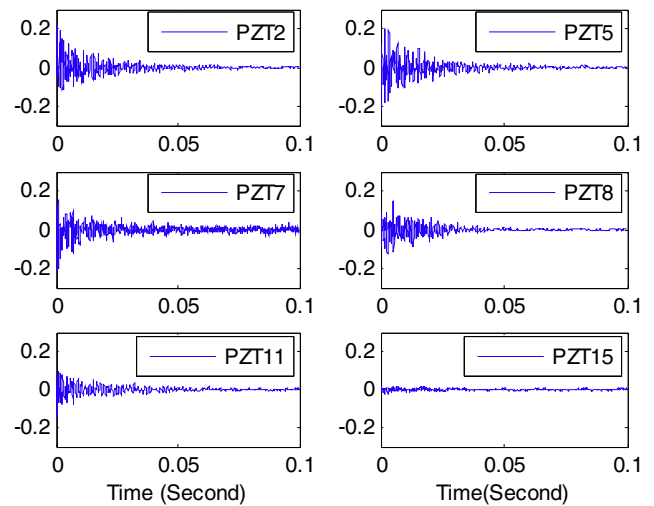
Figure 30. Impulse responses captured by smart aggregate sensors when the concrete frame is impacted at impact spot II.
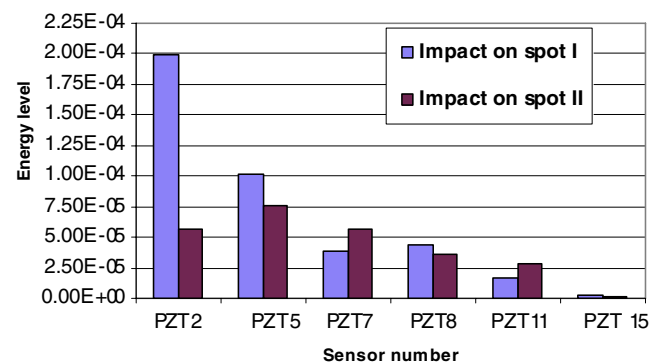
Figure 31. Energy level of the different sensors for the impact test.

From the experimental results, the following conclusions can be drawn: (1) when the concrete frame is impacted, the impulse response can be captured by the distributed smart aggregate sensors at different locations; (2) the amplitude of the sensor signal, sensor signal energy and energy distribution are related to the location of the impact spot. The closer the smart aggregate is to the impact spot, the higher the sensor signal amplitude and sensor energy will be.
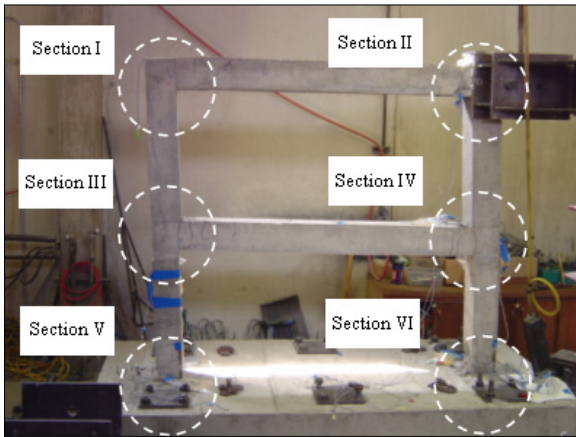
Figure 32. Concrete frame yields during the loading test.

(a) Cracks at section I   (b) Cracks at section II

(c) Cracks at section III   (d) Cracks at section IV

(e) Cracks at section V   (f) Cracks at section VI
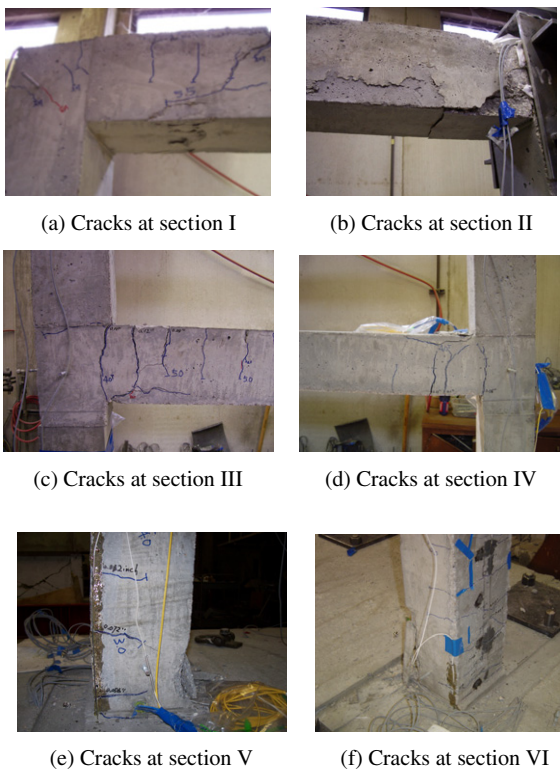
Figure 33. Damage status of the concrete frame after failure.

(c) *Experimental results of structural health monitoring.* During the structural health monitoring test, a push-over test is conducted. Before the appearance of a major crack, the test is in force control mode. After the appearance of a major crack, the test is set in the displacement control mode. During the force control mode, the load (force) is increased gradually at a fixed rate until cracking of the concrete frame. During the displacement control mode, the concrete frame is pushed by the hydraulic actuators to a certain position at a specified rate. These positions will be held for a certain time for data acquisition. After the push over, the concrete frame fails as shown in figure 32. The damage status at different locations is shown in figure 33.
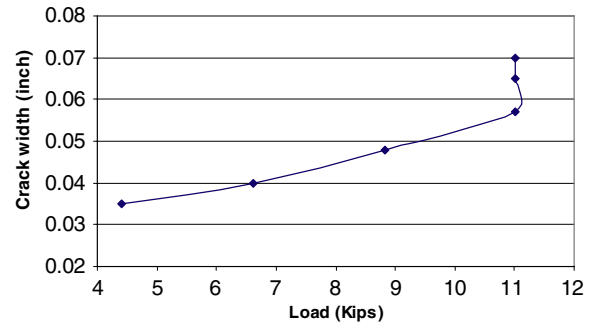
Figure 34. Crack width versus the load for a crack which first appears in the concrete frame.
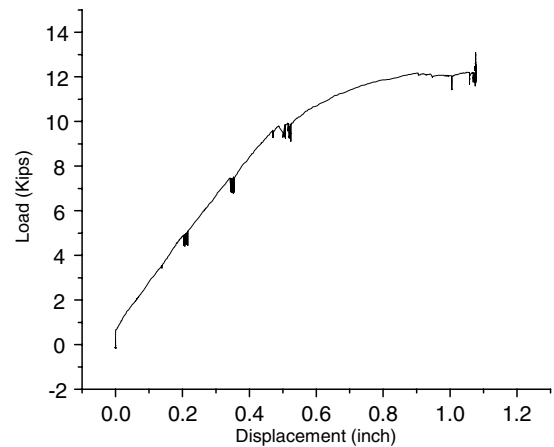
Figure 35. Load versus displacement for LVDT positioned at the top of the concrete frame.

The crack width for the first crack is observed by a microscope and it is plotted versus the load, as shown in figure 34, which clearly reveals that the relationship between the crack width and the load value is close to linear before the load value increases to 11.02 kips. After the load value reaches 11.02 kips, the crack width increases dramatically because of yielding of the reinforcing bars in the concrete frame and the relationship between crack width and load is highly nonlinear. In figure 35, the results of LVDT measurements show that the relationship between displacement and load is highly nonlinear after the load value reaches 11.02 kips. The LVDT experimental data also verified that the concrete frame yields at the load value of 11.02 kips.

During both load control and displacement control, the smart aggregates are utilized for the real-time structural health monitoring of the concrete frame. The detailed loading information at each structural health monitoring test has been shown in table 2. In the structural health monitoring algorithm, wavelet packet analysis is utilized as a signal-processing tool to analyze the sensor signals. The wavelet packet-based damage index matrix proposed previously has been used for the structural health monitoring of the concrete frame.

Figures 36 and 37 are the three-dimensional plots of the sensor-history damage index matrices with PZT3 and PZT14 as the actuator, respectively. Figure 37, with PZT3 as an actuator, shows the damage index increases greatly from test 3, with a load value of 6.61 kips, to test 4, with a load
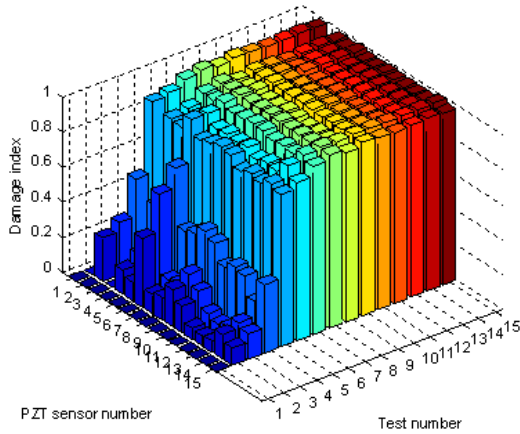
Figure 36. Sensor-history damage index matrix with PZT3 as an actuator.
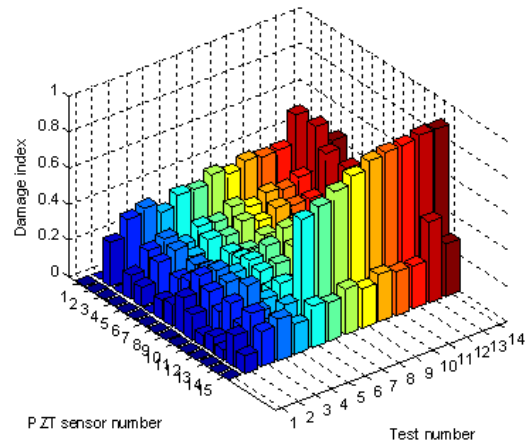
Figure 38. Sensor-history damage index matrix with PZT6 as an actuator.
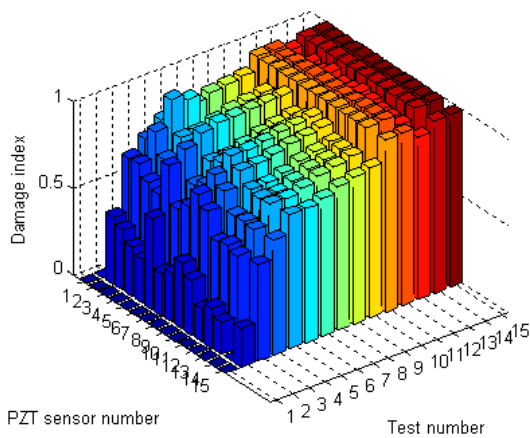
Figure 37. Sensor-history damage index matrix with PZT14 as an actuator.
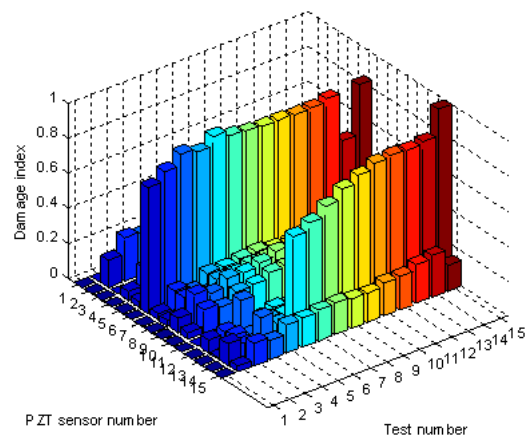
Figure 39. Sensor-history damage index matrix with PZT11 as an actuator.

value of 8.82 kips. In test 5, the damage index values of different sensors reach a critical value. Figure 37, with PZT14 as an actuator, shows the damage index values increase dramatically from test 2 to test 3, and reach greater values at test 4 for all sensors. Thus, in test 4, with a load value of 8.82 kips, the concrete frame already reached a critical damage situation at the root of one column. From the sensor-history damage index matrix results, the loading value of 8.82 kips is identified as the critical point, which is earlier than the critical point of 11.02 kips identified by the LVDT-based and microscope-based approaches. Figures 38 and 39 are the three-dimensional plots of the sensor-history damage index matrices with PZT6 and PZT11 as the actuator, respectively. Compared with the sensor-history damage index matrices with PZT3 and PZT14 as the actuator, the damage index values with PZT6 and PZT11 are smaller than those with PZT3 and PZT14 as an actuator. This shows that the damage status around PZT3 and PZT14 is more severe than PZT6 and PZT11. In both figures 38 and 39, PZT14 has a greater damage index value than other sensors. This also verifies PZT14 has a more severe damage status. It is noted that PZT14 is located in the plastic hinge region of the concrete frame.
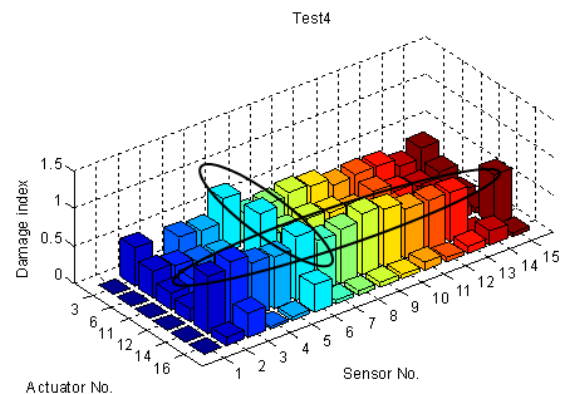
Figure 40. Actuator–sensor damage index matrix at test 4.

Figures 40 and 41 show the actuator–sensor damage index matrices for test 4 and test 5. In figure 40, it can be seen that, with PZT14 used as an actuator, the damage indexes of all the other sensors are close to the critical value. This means there is a critical damage status around PZT14 in test 4. PZT14 is located at the root of the column where the bending moment is greatest. From visual inspection, the damage situation at the
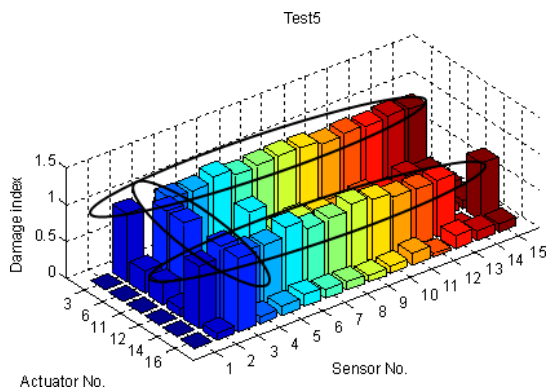
Figure 41. Actuator–sensor damage index matrix at test 5.

root of the column where PZT14 located is more severe than at other locations. From actuator–sensor damage index matrix results in figures 40 and 41, with PZT3 used as an actuator, the damage indexes of all the other sensors have greater values. Among the sensors, PZT6 always has greater damage index values than other sensors. This means that, around PZT3 and PZT6, there is severe damage. Visual inspection of the cracks on the concrete frame as shown in figure 33 verifies the damage index matrix results.

From the experimental results, the following conclusions can be drawn: the proposed sensor-history damage index matrix and actuator–sensor damage index matrix have demonstrated the damage status with the time-history and damage location information, respectively. The critical point captured by the proposed smart aggregate-based approach is ahead of the critical point captured by the traditional approaches based on microscopes and LVDTs.

6. Conclusions

As reported in this paper, an innovative, multi-functional smart aggregate has been developed to perform early-age concrete strength monitoring, impact detection and evaluation, and structural health monitoring for concrete structures. Comprehensive tests are conducted to evaluate these three functions of the smart aggregates. The experimental results of early-age strength monitoring show that, by monitoring the harmonic amplitude of the sensor signal, the strength development of concrete in early age can be monitored by a trained fuzzy correlation system. The experimental results of the impact tests show that the peak value of the sensor signal is proportional to the impact force. In the structural health monitoring test, wavelet packet analysis is used as a signal-processing tool. A damage index is proposed based on wavelet packet analysis. Two types of damage index matrices have been proposed to extract time-history and location information for damage. The experimental results of the structural health monitoring tests show that the proposed damage index can detect the critical damage situation earlier than conventional health monitoring approaches. The severity of the cracks and location information of the damage can also be evaluated by the proposed approach. The experimental programs successfully

demonstrate the multi-functionality of the smart aggregate. The proposed smart aggregate has the potential to be applied for multi-purpose evaluation of concrete structures from their early age and throughout their lifetime.

Acknowledgments

References

Abrams D P and Sozen M A 1979 Experimental study of frame–wall interaction in reinforced concrete structures subjected to strong earthquake motions *Civil Engineering Studies, Structural Research Series* Department of Civil Engineering, University of Illinois at Urbana-Champaign No. 460, p 400

Achenbach J D 1973 *Wave Propagation in Elastic Solids* (Amsterdam: Elsevier)

Ayotte E, Massicotte B, Houde J and Gocevski V 1997 Modeling the thermal stresses at early ages in a concrete monolith *ACI Mater. J.* **94** 577–87

Bernard R T, Galen K B, Joseph R C, Henry A A, Siamak S, Brian A K and Hans R Z 1988 Impact detection apparatus *US Patent Specification* 4745564

Bhalla S and Soh C K 2004 High frequency piezoelectric signatures for diagnosis of seismic/blast induced structural damages *NDT and E Int.* **37** 23–33

Chen X and Ansari F 2000 Fiber optic stress wave sensor for detection of internal flaws in concrete structures *J. Intell. Mater. Syst. Struct.* **10** 274–9

Demirboga R, Turkmen I and Karakoc M B 2004 Relationship between ultrasonic velocity and compressive strength for high-volume mineral-admixtured concrete *Cement Concrete Res.* **34** 2329–36

Desmon S and Linskey A 2006 Barge breaks loose, hits bridge on Severn *Baltimore Sun* (March 15)

Feld J and Carper K 1997 *Construction Failure* 2nd edn (New York: Wiley)

FHWA 2003 Recommendations for Bridge and Tunnel Security (September)

Fujii Y and Fujimoto H 1999 Proposal for an impulse response evaluation method for force transducers *Meas. Sci. Technol.* **10** N31–3

Gu H, Song G, Dhonde H, Mo Y L and Yan S 2006 Concrete early-age strength monitoring using embedded piezoelectric transducers *Smart Mater. Struct.* **15** 1837–45

Hassan A F and Sozen M A 1997 Seismic vulnerability assessment of low-rise buildings in regions with infrequent earthquakes *ACI Struct. J.* **94** 31–9

Hey F, Bhalla S and Son K C 2006 Optimized parallel interrogation and protection of piezo-transducers in electromechanical impedance technique *J. Intell. Mater. Syst. Struct.* **17** 457–68

Krauss M and Hariri K 2001 Assessment of concrete's stiffness development by means of ultrasonics *ISA TECH/EXPO Technology Update Conf. Proc.* vol 417, pp 7–15

Kreger M E and Sozen M A 1983 Study of the causes of column failures in imperial county services building during the 15 October 1979 Imperial Valley earthquake *Civil Engineering Studies, Structural Research Series* Department of Civil Engineering, University of Illinois at Urbana-Champaign No. 509, p 321

Lew H, Fattel S, Shaver J, Reinhold T and Hunt B 1979 *Investigation of Construction Failure of Reinforced Concrete Cooling Tower at Willow Island, W.V.* (Washington, DC: US Department of Labor, OSHA/National Bureau of Standards)

Lim Y Y, Bhalla S and Soh C K 2006 Structural identification and damage diagnosis using self-sensing piezo-impedance transducers *Smart Mater. Struct.* **15** 987–95

Lin Y B, Chang K C, Chern Jenn C and Wang L A 2004 The health monitoring of a prestressed concrete beam by using fiber Bragg grating sensors *Smart Mater. Struct.* **13** 712–8

Lu S and Xie H 2006 Real-time monitoring and simulating the load effects of smart CFRP-strengthened RC beams *Key Eng. Mater.* I **324/325** 129–32

Miller T, Hauser C J and Kundu T 2002 Nondestructive inspection of corrosion and delamination at the concrete–steel reinforcement interface *Proc. ASME Nondestructive Evaluation Engineering Division; American Society of Mechanical Engineers (Publication) NDE* vol 23, pp 121–8

Na W-B and Kund T 2003 Inspection of interfaces between corroded steel bars and concrete using the combination of a piezoelectric zirconate–titanate transducer and an electromagnetic acoustic transducer *Exp. Mech.* **43** 24–31

Naidu A S K and Bhalla S 2003 Damage detection in concrete structures with smart piezoceramic transducers *Proc. SPIE* **5062** 684–90

Nojavan S and Yuan F G 2006 Damage imaging of reinforced concrete structures using electromagnetic migration algorithm *Int. J. Solids Struct.* **43** 5886–908

NTSB 1994 Derailment of Amtrak Train No. 2 on the CSXT Big Bayou Canot Bridge Near Mobile, Alabama, Sept. 22, 1993 *NTSB Report Number: RAR-94-01*

NTSB 2004 *Safety Recommendations Issued by National Transportation Safety Board (NTSB)* Document No. H-04-29 and 30, Sept. 9

Okafor A C, Chandrashekhara K and Jiang Y P 1996 Delamination prediction in composite beams with built-in piezoelectric devices using modal analysis and neural network *Smart Mater. Struct.* **5** 338–47

Otani S and Sozen M A 1972 Behavior of multistory reinforced concrete frames during earthquakes *Beton* **392** 569

Park Y-J, Ang A H-S and Wen Y-K 1985 Seismic damage analysis of reinforced concrete buildings *J. Struct. Eng.* **111** 740–57

Park S, Ahmad S, Yun C-B and Roh Y 2006 Multiple crack detection of concrete structures using impedance-based structural health monitoring techniques *Exp. Mech.* **46** 609–18

Raju V, Park G and Cudney H H 1999 Impedance-based health monitoring of composite reinforced structures *9th Int. Conf. on Adaptive Structures and Technologies* pp 448–57

Ren L, Li H, Li X, Zhou J and Xiang L 2006 Application of FBG sensors in rolled concrete dam model *The International Society for Optical Engineering, Smart Structures and Materials 2006—Sensors and Smart Structures Technologies for Civil, Mechanical, and Aerospace Systems; Proc. SPIE* **6174** 36

Saafi M and Sayyah T 2001 Health monitoring of concrete structures strengthened with advanced composite materials using piezoelectric transducers *Composites* B **32** 333–42

Saiidi M and Sozen M A 1981 Simple nonlinear seismic analysis of R/C structures *ASCE J. Struct. Div.* **107** 937–52

Soh C H, Tseng K K, Bhalla S and Gupta A 2000 Performance of smart piezoceramic patches in health monitoring of a RC bridge *Smart Mater. Struct.* **9** 533–42

Song G, Gu H, Mo Y L, Hsu T T C and Dhonde H 2007a Concrete structural health monitoring using embedded piezoceramic transducers *Smart Mater. Struct.* **16** 959–68

Song G, Olmi C and Gu H 2007b An overheight vehicle–bridge collision monitoring system using piezoelectric transducer *Smart Mater. Struct.* **16** 462–8

Staszewski W J, Worden K, Wardle R and Tomlinson G R 2000 Fail-safe sensor distributions for impact detection in composite materials *Smart Mater. Struct.* **9** 298–303

Sun F P, Chaudhry Z, Rogers C A and Majmundar M 1995 Automated real-time structure health monitoring via signature pattern recognition *Proc. SPIE* **2443** 236–47

Tedesco J 2006 Presentation of nanotechnology in cementitious materials—objectives of workshop *National Science Foundation Workshop on Nanomodification of Cementitious Materials: Portland Cement Concrete and Asphalt Concrete (University of Florida, Gainesville, FL, Aug. 2006)*

Tseng K K and Wang L 2004 Smart piezoelectric transducers for *in situ* health monitoring of concrete *Smart Mater. Struct.* **13** 1017–24

Tseng K K-H and Naidu A S K 2002 Non-parametric damage detection and characterization using smart piezoceramic material *Smart Mater. Struct.* **11** 317–29

Voigt Th, Grosse Ch U, Sun Z, Shah S P and Reinhardt H-W 2005 Comparison of ultrasonic wave transmission and reflection measurements with P- and S-waves on early age mortar and concrete *Mater. Struct.* **38** 729–38

Wang C-H and Wen Y-K 2000 Evaluation of pre-Northridge low-rise steel buildings. I: modeling *J. Struct. Eng.* **126** 1160–8

Wen Y K 2001 Reliability and performance-based design *Struct. Safety* **23** 407–28

Yang Y C and Han K S 2002 Damage monitoring and impact detection using optical fiber vibration sensors *Smart Mater. Struct.* **11** 337–45

Zhang W, Gao J, Shi J, Cui H and Zhu H 2006 Health monitoring of rehabilitated concrete bridges using distributed optical fiber sensing *Comput.-Aided Civil Infrastruct. Eng.* **21** 411–24

Zhao X and Li H 2006 Health monitoring of reinforced concrete frame-shear wall using piezoceramic transducer *J. Vib. Shock* **25** 82–4